

# Ontogeny of Poly(ADP-Ribose) Polymerase-1 in Lung and Developmental Implications

Robert Ertsey, Cheryl J. Chapin, Joseph A. Kitterman, and Louis M. Scavo

Cardiovascular Research Institute, and Department of Pediatrics, University of California, San Francisco, California

Poly(ADP-ribose) polymerase 1 (PARP-1) is the predominant NAD-dependent modifying enzyme in DNA repair, transcription, and apoptosis; its involvement in development has not been defined. Here, we report expression and cellular localization of PARP-1 in developing rat and human fetal lung, *in vivo* and in explant culture, and effects of inhibiting PARP-1 activity on lung surfactant protein (SP) expression. PARP-1 was expressed as 113-kD (p113) and 85-kD (p85) fragment in both rat and human lung. In rat lung, p113 content by Western was maximal at Embryonic Days 16–18, decreased sharply by Embryonic Day 20, and continued to decrease postnatally. p85 level was constant in the fetus and decreased postnatally. In human fetal lung, both PARP-1 mRNA expression and protein content changed little between 15 and 24 wk. Immunohistochemistry for PARP-1 in Embryonic Day 18 rat lung showed predominantly nuclear staining in most cells. In later gestation and postnatally, PARP-1 staining was primarily cytoplasmic and progressively restricted to a subset of cells, mainly bronchial epithelial and smooth muscle cells. Cell subfractionation showed that p113 localized to nucleus and p85 to cytoplasm. Inhibition of PARP-1 activity by 5-iodo-6-amino-1,2-benzopyrone in fetal rat lung explant culture did not affect SP-A and -B mRNA, but significantly increased SP-C mRNA. These findings indicate that in lung (i) PARP-1 is abundantly expressed during fetal development; (ii) p113 and p85 levels are differentially regulated; (iii) PARP-1 undergoes complex developmental changes in cellular and subcellular expression, including extensive cytoplasmic localization; and (iv) inhibition of PARP-1 activity differentially affects expression of SPs.

Poly (ADP-ribose) polymerase-1 (PARP-1) is a 113-kD enzyme that catalyzes the covalent attachment of ADP-ribose units [poly (ADP-ribosyl)ation] to acceptor molecules, using NAD<sup>+</sup> as a substrate. Studies over the last decade indicate that PARP-1 has a prominent role in the process of apoptosis (1). Because PARP-1 is a target of caspases, such as caspase 3, which are important for execution of the apoptotic pathway, evaluating PARP-1 cleavage products by Western analysis has been a useful way of confirming and following the process of apoptosis (2). Additionally, other studies have been aimed at defining the role PARP-1 plays in a broad range of biological processes important for the genomic integrity, differentiation, and functioning of nonapoptotic cells (3).

The gene encoding PARP-1 is highly conserved and present in almost all eukaryotes, which is consistent with its playing an important role in fundamental biological events (4). Although the exact physiologic roles remain to be defined, PARP-1 and

poly (ADP-ribosyl)ation have been associated with a number of functions, including DNA repair (5) and replication (6, 7), cell cycle regulation (8), cell proliferation (9), differentiation (10–12), and cell death (13, 14). The drosophila PARP-1<sup>-/-</sup> phenotype develops to the end of embryogenesis but does not grow into the adult fly, indicating an essential developmental role for PARP-1 in this model (15). The mouse PARP-1 knockout has provided limited insight into the involvement of PARP-1 in mammalian development (16–18) due to the redundancy of poly (ADP-ribosyl)ating enzymes with similar biochemical activity (19); multiple knockouts, with poly(ADP-ribosyl)ation completely abolished, have not been described. Thus, the role of PARP-1 in mammalian developmental events, including differentiation and programmed cell death, remains to be established.

We previously demonstrated that apoptosis is a normal component of development in rat and human fetal lung (20). PARP-1 has been implicated in the induction of apoptosis (1), and its cleavage by caspases into specific fragments has been viewed as a critical event in this process (21). In preliminary experiments using a fetal lung explant culture system in which there is accelerated type II cell maturation (22) and increased apoptosis (20), we found that PARP-1 content was highly regulated, and that its catabolism could not be explained solely by apoptotic caspase cleavage. This suggested that PARP-1 expression may undergo developmental regulation in the lung. *In vitro* studies of adipocyte differentiation have shown that PARP-1 expression and activity are regulated at the onset of differentiation (12). In the *in vivo* chick limb differentiation model, PARP-1 activity shows developmental regulation (11). However, the ontogenic expression and cellular localization of PARP-1 in mammalian development in general, and in lung specifically, have not been described. Determining the temporal expression and spatial distribution of PARP-1 is fundamentally important as a first step to understanding the physiologic functions of PARP-1.

This study was undertaken to characterize PARP-1 expression and cellular localization in rat fetal and postnatal lung (RFL and RPNL) and human fetal lung (HFL). The results demonstrate that PARP-1 is expressed in RFL, RPNL, and HFL and that PARP-1 is developmentally regulated *in vivo* and *in vitro*. In addition, inhibiting PARP-1 activity in late gestation differentially affects the expression of surfactant protein (SP)-A, -B, and -C mRNA. A preliminary report has appeared (23).

## Materials and Methods

### Fetal and Postnatal Rat Lung and Explant Culture

All studies were approved by the Committee on Animal Research at the University of California, San Francisco. Time dated pregnant Sprague Dawley rats were obtained from Charles River Labs (Gilroy, CA) and housed at the UCSF Animal Care Facility. We examined specimens from fetal rats delivered at Gestational Days 16–22 (Embryonic Days 16 to 22) ( $n = 19$  pregnant rats) and from postnatal rats ages 1, 4, 7, 21 d and 3 mo ( $n = 14$  rats). Pregnant females and their fetuses were anesthetized with a mixture of ketamine (87.5 mg/kg) and xylazine (1.25 mg/kg) intramuscularly. Fetuses were delivered by hysterotomy at Embryonic Days 16–22, pithed, weighed, and the lungs dissected. After fetuses had been delivered, dams were killed by intracardiac

(Received in original form June 27, 2003 and in revised form December 19, 2003)

Address correspondence to: Louis M. Scavo, M.D., Department of Neonatology, Children's National Medical Center, 111 Michigan Avenue, Washington, D.C. 20010. E-mail: lscavo@cnmc.org

Abbreviations: dithiothreitol, DTT; human fetal lung fibroblasts, HFL; poly(ADP-ribose) polymerase 1, PARP-1; phosphate-buffered saline, PBS; rat fetal lung fibroblasts, RFL; reverse transcriptase–polymerase chain reaction, RT-PCR; surfactant protein, SP; Tris-buffered saline, TBS.

Am. J. Respir. Cell Mol. Biol. Vol. 30, pp. 853–861, 2004  
Originally Published in Press as DOI: 10.1165/rcmb.2003-0248OC on January 30, 2004  
Internet address: www.atsjournals.org

injection of 1 ml of euthanasia solution containing 67 mg/ml pentobarbital, followed by bilateral pneumothoraces. Postnatal rats were killed with pentobarbital and the lungs dissected. Some lungs were promptly frozen in liquid nitrogen and stored at  $-70^{\circ}\text{C}$  for use in biochemical studies. Other lungs were fixed for microscopy by immersion in freshly prepared 4% paraformaldehyde in 0.1 M phosphate-buffered saline (PBS), pH 7.4 overnight. Lungs were cryoprotected with 30% sucrose in 4% paraformaldehyde/0.1 M PBS, pH 7.4 at  $4^{\circ}\text{C}$  overnight. Individual lobes were placed in O.C.T. compound from Tissue-Tek (Elkhorn, IN), frozen under liquid nitrogen, and stored at  $-70^{\circ}\text{C}$ . For explant culture, lungs were minced into 1-mm cubes and cultured in Waymouth +10% fetal bovine serum with either the specific inhibitor of PARP activity, 5-iodo-6-amino-1,2-benzopyrone (INH<sub>2</sub>BP) (24) (kindly provided by Dr. E. Kun, University of California, San Francisco), or DMSO vehicle in 95%/5% CO<sub>2</sub> as previously described (22). The tissue was harvested at times indicated, snap frozen, and stored at  $-70^{\circ}\text{C}$ .

### HFL and Explant Culture

All studies were approved by the Committee on Human Research at the University of California, San Francisco. For HFL, pathologic specimens were available only during the canalicular stage (15–24 wk gestation). As a complement to the *in vivo* HFL samples, we used an HFL explant system that shows accelerated maturation of type II cells (22, 25, 26), architectural remodeling (22), and an increased rate of interstitial apoptosis (20). Lung tissue was harvested on wet ice and stored overnight at  $4^{\circ}\text{C}$  in serum-free Waymouth MB 752/1 from GIBCO-BRL (Gaithersburg, MD) before processing. Lung tissue was minced under sterile conditions into 1-mm cubes and cultured in serum-free Waymouth MB 752/1 medium in 95% air/5% CO<sub>2</sub>, as previously described (22). The tissue was harvested at times indicated, snap frozen, and stored at  $-70^{\circ}\text{C}$ .

### Protein Extraction and Western Immunoblot Analysis

Frozen tissue (HFL and RFL) was transferred to 3× volumes of homogenization buffer (0.5% NP-40, 0.3 M NaCl, 0.1 mM EDTA, 20 mM HEPES, 10% glycerol, 1 mM dithiothreitol [DTT], and 2% protease inhibitor cocktail) (Sigma, St. Louis, MO) and Dounce homogenized on ice. Samples were sonicated for 20 s on ice on a setting of 30% power followed by mixing at  $4^{\circ}\text{C}$  for 60 min on a rocker platform. The samples were centrifuged for 5 min and the supernatant stored at  $-70^{\circ}\text{C}$ . An aliquot was removed to determine protein concentration using the Bradford assay (Bio-Rad, Richmond, CA). Equal amounts of protein extract were mixed with 2× sample buffer containing 6 M urea (0.35 M TrisCl, 4% SDS, 20% glycerol, 2.0% betamercaptoethanol, pH 6.8) and incubated at  $60^{\circ}\text{C}$  for 15 min. Proteins were separated on a 10% SDS-PAGE with a 4% stacking gel and blotted electrophoretically onto 0.45 micron nitrocellulose (MSI, Westboro, MA). After blocking in freshly prepared 5% milk-TRIS-buffered saline (TBS, pH 7.4), the blots were incubated with C2-10 anti-PARP-1 mAb (PharMingen, San Diego, CA) diluted 1:250 in 2.5% milk-TBS, for 2 h at room temperature with rocking. The C2-10 mAb binds both the full-length 113-kD PARP-1 and 85-kD apoptotic cleavage fragment (27). The blots were washed extensively with TBS-Tween-20 (0.05%, TBS-T) and incubated with anti-mouse IgG, horseradish peroxidase conjugated (Amersham, MA), diluted 1:2,000 in 2.5% milk-TBS, for 1 h at room temperature with rocking. Membranes were washed with TBS-T and developed with an enhanced chemiluminescence detection kit (ECL+; Amersham International, Amersham, UK). Images were recorded on Hyperfilm MP (Amersham) or captured using a phosphorimager system (Storm 840; Molecular Dynamics, Sunnyvale, CA) and analyzed using Image-Quant Software (Molecular Dynamics).

### Immunohistochemistry

Immunohistochemistry was performed on 3  $\mu\text{m}$  sections of fixed, cryoprotected rat lung using primary antibodies to PARP-1 and RTII<sub>70</sub>, a protein specific in the lung to the apical surface of rat type II cells (28). For PARP-1, sections were treated with 1% H<sub>2</sub>O<sub>2</sub> for 10 min at room temperature and washed with TBS. Antigen retrieval was performed in 10 mM Na Citrate, pH 6.0 (target retrieval solution; Dako, Carpinteria, CA) at  $95^{\circ}\text{C}$  for 10 min followed by a cooling phase of 20 min at room temperature. Sections were washed with TBS and incubated with blocking solution (TBS/0.1% BSA/0.3% Triton X-100/10% rabbit se-

rum) for 1 h at room temperature to block nonspecific binding. The tissue sections were incubated with C2-10 mAb, diluted 1:500 in TBS/0.1% BSA/0.3% Triton/1.5% rabbit serum, at  $4^{\circ}\text{C}$  overnight. After extensive washing in TBS/0.1% BSA/0.3% Triton X-100, the sections were incubated with rabbit anti-mouse IgG biotin-conjugated for 1 h at room temperature. For histochemical localization of PARP-1, we used the Vectastain ABC kit (Vector Laboratories, Burlingame, CA) for 3,3'-diaminobenzidine (DAB) staining of tissue sections. To label nuclei, sections were counterstained with Gill's No. 2 hematoxylin (Sigma). Sections were air dried and mounted with Glycergel (Dako) and analyzed with a Leitz Orthoplan 2 microscope. For RTII<sub>70</sub>, sections were treated as previously described (28) with the modification that, for detection by direct immunofluorescence, the sections were incubated with isotype specific goat anti-mouse IgG<sub>3</sub> Alexa Fluor 488 (Molecular Probes, Eugene, OR). The antigen retrieval process, used for PARP-1 and described above, interfered with detection of RTII<sub>70</sub>. Therefore, to co-localize PARP and RTII<sub>70</sub>, serial sections were examined using the Leitz Orthoplan 2 microscope.

For confocal microscopy, sections were prepared as described above for PARP-1 except that, instead of diaminobenzidine, a 1:500 dilution of FITC-conjugated avidin (Jackson ImmunoResearch, West Grove, PA) in PBS (pH 7.4) was added for 30 min at room temperature followed by extensive washing. Sections were counterstained with propidium iodide (10  $\mu\text{g}/\mu\text{l}$ ; Sigma) for 15 min to label all nuclei, washed sequentially with PBS and distilled H<sub>2</sub>O, and coverslipped using 1,4-diazabicyclo(2,2,2)octane (DABCO) (Sigma).

### Cellular Subfractionation

Cells were subfractionated as previously described by Bohinski and coworkers (29) with the following modifications. Rat lungs (21pd) were finely powdered in liquid nitrogen using mortar and pestle and Dounce homogenized on ice in 4 vols of isotonic buffer (10 mM HEPES pH 7.9, 10 mM KCl, 0.1 mM EDTA, 1.5 mM MgCl<sub>2</sub>, 0.2% Nonidet P-40, 1 mM DTT, and proteinase inhibitor cocktail; Sigma). Nuclei were spun down at  $720 \times g$  for 5 min at  $4^{\circ}\text{C}$ , and the supernatant was saved for the cytoplasmic fraction. The pellet of nuclei was resuspended in 4 vols of buffer (20 mM HEPES pH 7.9, 420 mM NaCl, 0.1 mM EDTA, 1.5 mM MgCl<sub>2</sub>, 25% glycerol, 1 mM DTT, and protease inhibitor cocktail), and both cytoplasmic and nuclear fractions were sonicated at 30% power for 20 s on ice. The nuclear fraction was centrifuged at  $16,000 \times g$  for 10 min at  $4^{\circ}\text{C}$  and the supernatant used for further analysis.

### Isolation and Analysis of Lung RNA

Total RNA was isolated from HFL by the RNazol method (CINNA/BIOTECX Laboratories, Friendswood, TX). Tissue samples were removed from  $-70^{\circ}\text{C}$ , homogenized directly in RNazol solution, extracted with chloroform-isoamyl alcohol, centrifuged at  $14,000 \times g$  at  $4^{\circ}\text{C}$  for 15 min, and precipitated with isopropanol at  $-20^{\circ}\text{C}$ . RNase inhibitor RNasin (Promega, Madison, WI) was added directly onto the final RNA pellet (40 U/pellet) to inhibit any residual RNase activity. RNA pellets were resuspended in 1 mM DTT and the quantity and purity of RNA was determined by optical density at 260 and 280 nm. The quality and quantitation of the RNA was verified by electrophoresis of 0.5  $\mu\text{g}$  aliquot in a 1% agarose-formaldehyde gel that was stained with ethidium bromide to visualize the 18S and 28S rRNA bands.

Multiplex reverse transcriptase-polymerase chain reaction (RT-PCR) was used for the analysis of human PARP-1, rat SP-A, SP-B, and SP-C mRNA in combination with 18S rRNA using Competimer technology (Ambion, Austin, TX) as previously described (28). Total RNA was reverse transcribed using random primers. cDNA was amplified with specific oligonucleotides for rat SP-A, SP-B, and SP-C as previously described (30) and for human PARP-1 as follows: 5'-GAAGCTCAGAGAACCCATCC (GenBank nm001618, bp# 372–391) (antisense) and 5'-AAGCTCTATCGAGTCGAGTACG (bp# 178–199) (sense). For each gene we determined the linear range of amplification and the optimal 18S Primer: Competimer ratio (PARP-1 = 1:9, SP-A = 2:8, SP-B = 2:8, and SP-C = 2:8). Radiolabeled PCR products were produced using direct incorporation of  $\alpha$ -<sup>32</sup>P-dCTP (3,000 Ci/mmol; NEN, Boston, MA) during amplification (18 cycles for PARP-1 and SP-A, 17 cycles for SP-B and SP-C). PCR products were resolved on 6% polyacrylamide gel containing 8 M urea. After drying the gel, PCR products were quantified using the Storm 840 phosphorimager equipped

with a blue fluorescence/chemifluorescence detector and ImageQuant software (Molecular Dynamics).

### Statistical Analysis

Student's unpaired *t* test was used for comparing group values from the rat developmental series. Regression analysis was used to analyze PARP-1 protein levels during development in rat. HFL culture values were compared by ANOVA using Bonferroni/Dunn *post hoc* test. Data are presented as ratios  $\pm$  SE, except where stated otherwise. All statistical analyses were done using Statview (Abacus Concepts, Berkeley, CA). *P* values < 0.05 were considered significant.

## Results

### Content of PARP-1 Protein in Fetal and Postnatal Rat Lung

The lung content of 113-kD PARP-1 (p113) (expressed as a ratio to Postnatal Day 1) was maximal at Embryonic Days 16–18, decreased sharply from  $3.3 \pm 0.7$  (mean  $\pm$  SD) at Embryonic Day 18 to  $1.08 \pm 0.1$  at Embryonic Day 20 ( $P < 0.001$ ), and continued to diminish in the postnatal period, becoming minimally detectable in the adult (Figures 1A and 1B). For the entire period, Embryonic Day 16 to adulthood, the decrease in p113 was significant ( $n = 28$ ,  $R^2 = 0.27$ ,  $P < 0.005$ ). The 85-kD fragment (p85) was also detected (Figure 1A), consistent with observations that both fetal (20) and neonatal rat lung undergo apoptosis (31–33). However, the content of p85 did not increase proportionately to the decrease in p113 in late gestation (Figure 1B); p85 content was relatively constant prenatally ( $n = 16$ ,  $R^2 = 0.003$ ) and decreased after birth through adulthood ( $n = 16$ ,  $R^2 = 0.86$ ,  $P < 0.001$ ).

### Cellular Localization of PARP-1 during Development

To characterize expression at the cellular level, PARP-1 protein was localized in fetal and postnatal rat lung by immunohistochemistry. At Embryonic Day 16 (pseudoglandular phase), intense nuclear staining was evident in peripheral parenchyma and

in cells along the branching epithelial tubules (Figure 2A); both groups of cells also showed weak cytoplasmic immunoreactivity. Weaker nuclear staining was observable in most other cells. Consistent with previous observations (3), nucleated erythrocytes displayed little or no immunoreactivity (Figures 2A and 2B).

A striking change was seen at the transition between the pseudoglandular and the canalicular stage (Embryonic Day 18), with almost all cells showing intense nuclear stain (Figure 2B). At Embryonic Day 20, the transition between canalicular and saccular stages, there was differentially decreased staining between cell compartments, with interstitial cells showing reduced nuclear staining, whereas most epithelial cells displayed intense nuclear immunoreactivity (Figure 2C). At Embryonic Day 22, there was decreased staining in all cell types, although many epithelial cells continued to show marked PARP-1 signal (Figure 2D). On Postnatal Day 1, PARP-1 nuclear immunostaining was significantly diminished in most cells of the parenchyma (Figure 2E). Lungs from Postnatal Day 4, Postnatal Day 7, and Postnatal Day 21 showed minimal staining, with most cells having low or undetectable PARP-1 expression (Figures 2F and 2G), except for rare epithelial cells (Figure 2G). In contrast to the overall decrease in expression postnatally, most smooth muscle cells began to display marked PARP-1 staining on Postnatal Day 1 (Figure 3B). In general, adult lung showed weak PARP-1 staining, although macrophages were markedly positive (Figure 2H).

### Subcellular Localization of PARP-1 during Development in Rat Lung

In conducting airway epithelial cells PARP-1 immunostaining shifted from primarily nuclear at ed18 (Figure 3A) to cytoplasmic perinuclear at Postnatal Day 1 (Figure 3B), which persisted, along with weaker nuclear staining, in adult lung (Figure 3C). The smooth muscle cells that began to display marked PARP-1 staining on Postnatal Day 1 demonstrated predominantly cytoplasmic localization of PARP-1 (Figure 3B). The distribution and appearance of cytoplasmic PARP-1 staining was variable in different cell types. Intense, non-nuclear staining was observed in dividing cells, in apparent association with mitotic-phase chromatin (Figure 4A). In smooth muscle cells, PARP-1 cytoplasmic immunoreactivity was evenly distributed and appeared to be arrayed in linear patterns (Figure 4B), whereas in airway epithelial cells granular, perinuclear staining was predominant. Macrophages showed abundant cytoplasmic staining that appeared to fill most of the cytoplasm (Figure 4C).

### Confocal Microscopy

To determine whether the postnatal perinuclear signal observed in conducting airway epithelial cells in rat lung was intra- or extranuclear, we performed confocal microscopy on fluorescently labeled cryosections. The results showed that the perinuclear distribution in Postnatal Day 1 lung was cytoplasmic and the intensity of staining much stronger than in the nucleus (Figure 5).

### Subcellular Fractionation in Rat Lung

To characterize further the cytoplasmic distribution of PARP-1 in postnatal lung, Postnatal Day 21 lungs were subfractionated into nuclear and cytoplasmic fractions and analyzed by Western immunoblot. As shown in Figure 6, p113 localized to the nuclear and p85 to the cytoplasmic compartments.

### Expression of PARP-1 mRNA and Protein in HFL *In Vivo*

HFL specimens were available from 15–24 wk of gestation, which represents primarily the canalicular stage of lung development. Expression of PARP-1 mRNA in HFL was relatively constant

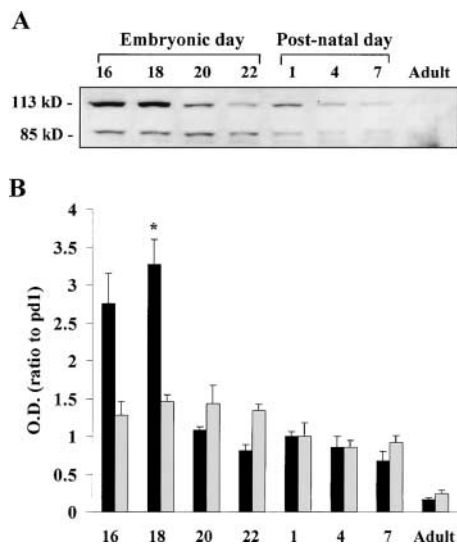


**Figure 1.** PARP-1 content in fetal and postnatal rat lung. (A) PARP-1 protein detected by Western immunoblot. Fifteen or 30  $\mu$ g of total protein/lane were subjected to electrophoresis on SDS-10% PAGE, transferred, and immunoblotted. Data are representative of four observations. (B) Optical densitometry of Western immunoblots. Values are expressed as ratio to Postnatal Day 1. Values are means  $\pm$  SE; Fetal:  $n = 4$  fetuses from different pregnant rats; postnatal:  $n = 4$  rats. Filled bars, 113 kD; shaded bars, 85 kD. \* $P < 0.05$  compared with Postnatal Day 1. See text for discussion.

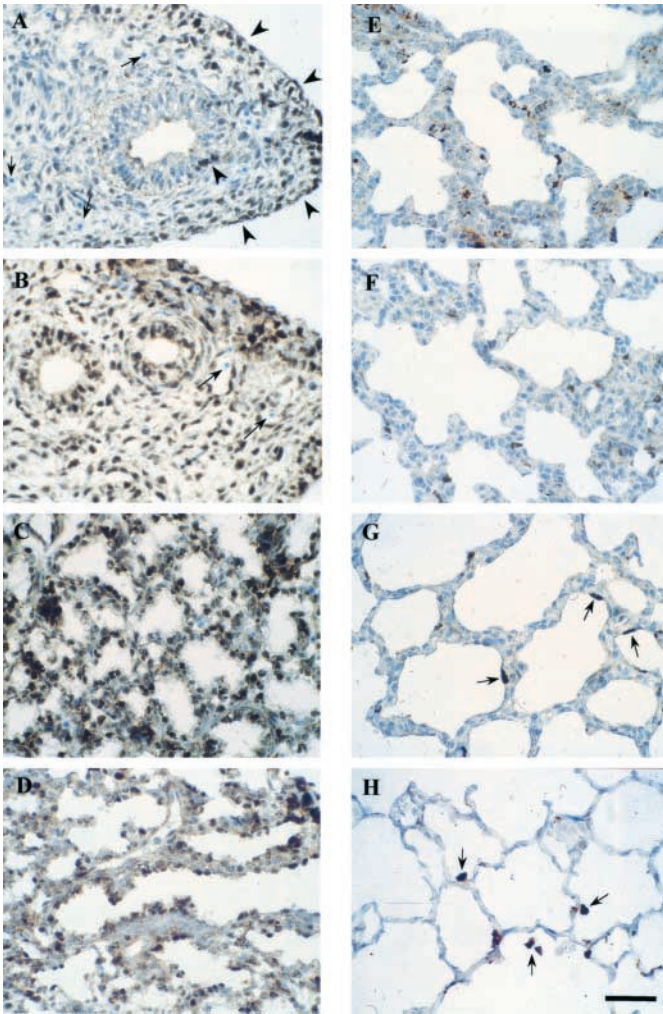


**Figure 2.** Immunohistochemical localization of PARP-1 in the parenchyma of fetal and postnatal rat lung. Positive signal was visualized by dark brown color. (A) Embryonic Day 16: intense nuclear PARP-1 signal observed in peripheral cells and epithelial tubules (arrowheads), moderate staining in most other cells, nucleated erythrocytes negative (arrows). (B) Embryonic Day 18: intense nuclear signal in almost all cells, nucleated erythrocytes negative (arrows). (C) Embryonic Day 20: decreased staining in interstitial cells, most epithelial cells showing intense signal. (D) Embryonic Day 22: decreased staining overall, but many epithelial cells still markedly positive. (E) Postnatal Day 1: substantially decreased signal in all cell types. (F) Postnatal Day 4: further decrease in the postnatal period, with positive signal limited to a few epithelial cells and alveolar macrophages. (G) Postnatal Day 7 (arrows point to epithelial cells). (H) Adult (arrows point to macrophages). Data were replicated in four separate experiments. Bar = 50  $\mu$ m.

from 15 through 22 wk gestation, followed by an apparent decrease at 24 wk (Figure 7A). PARP-1 protein was expressed predominantly as p113 and showed no clear pattern of change from 13.5 wk through 20 wk, followed by a trend of modestly reduced levels at 21 and 22.5 wk (Figure 7B).

#### PARP-1 Expression in HFL Explant Culture

In HFL explant culture, p113 content was relatively constant over the first 2 h, decreased significantly at 4 h ( $P < 0.02$  compared with 0 h), and was minimally detectable at 24 h ( $P < 0.005$  compared with 0 h) (Figures 8A and 8B). p85 was detectable in the preculture sample, in accordance with previous observations

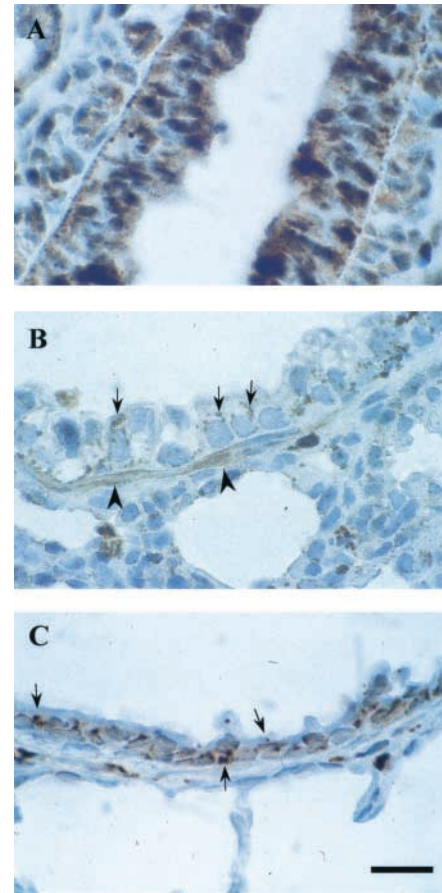


**Figure 3.** Cellular and subcellular localization of PARP-1 in conducting airway epithelial cells in fetal and postnatal rat lung. PARP-1 expression was detected by immunohistochemistry; positive signal was visualized by dark brown color. (A) Embryonic Day 18: intense nuclear PARP-1 signal, with more moderate cytoplasmic staining. (B) Postnatal Day 1: reduced staining in epithelial cells and a marked shift from nuclear to cytoplasmic, perinuclear granules (arrows); increased expression in smooth muscle cells (arrowheads). (C) Adult: positive PARP-1 staining in epithelial cells, with perinuclear granules evident (arrows). Bar = 20  $\mu$ m.

that HFL undergoes apoptosis (20), and tended to increase at 2 and 4 h ( $P = 0.25$  and 0.46, respectively, versus 0 h control), consistent with apoptosis in a subset of interstitial cells (20). However, the striking reduction in p113 content by 24 h did not result in a proportional increase in p85 levels.

#### Effect of the PARP-1 Inhibitor, INH<sub>2</sub>BP, on Surfactant Protein mRNA Expression

We analyzed the effect of the specific PARP-1 inhibitor, INH<sub>2</sub>BP, on mRNA expression for SP-A, SP-B, and SP-C in late gestation fetal rat lung. Embryonic Day 21 lungs were cultured as explants in the presence of 200  $\mu$ M INH<sub>2</sub>BP and harvested at 0, 4, 24, and 48 h. Results are shown in Figure 9. INH<sub>2</sub>BP did not affect SP-A mRNA expression. With INH<sub>2</sub>BP, SP-B mRNA content showed no change at 4 h and 24 h, and tended to increase at 48 h ( $P = 0.05$ ). With INH<sub>2</sub>BP, SP-C mRNA expression was unchanged at 4 h but increased significantly at 24 h ( $P < 0.05$ ) and at 48 h ( $P < 0.05$ ) compared with their respective control values.

#### Effect of the PARP-1 Inhibitor, INH<sub>2</sub>BP, on PARP-1 Content and Localization

Because PARP-1 expression is regulated during fetal development, the effects observed in SP mRNAs may have been due

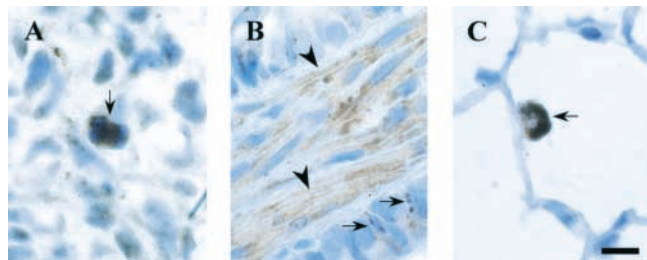


Figure 4. Cytoplasmic immunohistochemical localization of PARP-1 in fetal and postnatal rat lung. (A) Dividing cell at Embryonic Day 16 (arrow). (B) Airway smooth muscle cells at Postnatal Day 21 (arrowheads), typical of almost all smooth muscle cells; perinuclear signal in epithelial cells (arrows). (C) Alveolar macrophage in adult, typical of most macrophages (arrow) (see Figure 2H). Bar = 10 μm.

to effects by INH<sub>2</sub>BP on PARP-1 expression rather than activity. To clarify this issue, PARP-1 content and localization were analyzed in Embryonic Day 21 RFL explants cultured as above. Results are shown in Figure 10. In control cultures, p113 content tended to decrease at 4 h to ~50% of the content at time zero ( $P = 0.05$ ) and showed little further change at 24 h and 48 h (Figure 10A). Compared with control, INH<sub>2</sub>BP did not significantly affect p113 content at any time point. Similarly, p85 content decreased in control cultures at 4 h ( $P < 0.05$ ) and showed no further change at 24 h and 48 h (Figure 10B). As with p113, compared with control, INH<sub>2</sub>BP did not significantly affect p85 content at any time point. Figure 10C shows that by immunohistochemistry, PARP-1 colocalized with RTII<sub>70</sub>, a protein specific in the lung to alveolar type II cells, in control and INH<sub>2</sub>BP cultures at 48 h. Findings were similar after 4 and 24 h of culture (results not shown).

**Discussion**

The prevailing opinion has been that PARP-1 is a uniformly abundant nuclear enzyme activated by random DNA breaks

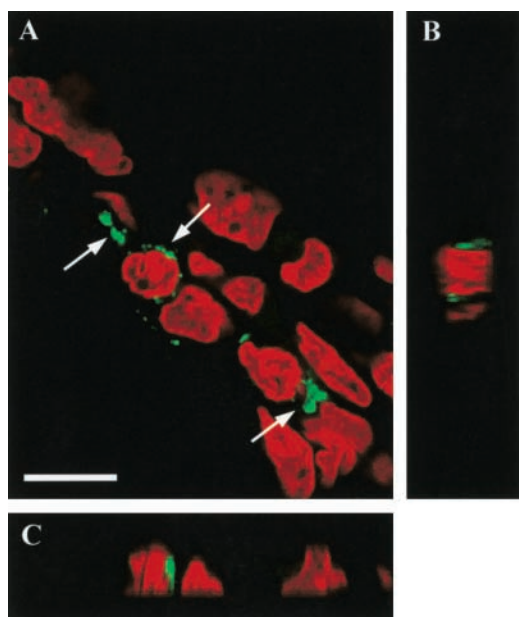


Figure 5. Immunofluorescent subcellular localization of PARP-1 in rat lung parenchyma on Postnatal Day 1 by confocal microscopy. Green: PARP-1; red: nuclei stained with propidium iodide. (A) xy; (B) yz; (C) xz. Arrows indicate perinuclear cytoplasmic localization of PARP-1. Bar = 10 μm.

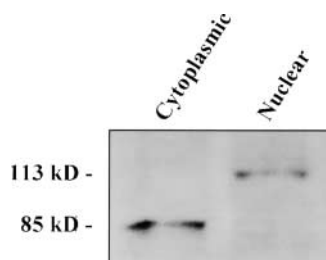


Figure 6. Analysis of p113 and p85 distribution by subcellular fractionation in postnatal 21 d rat lung. Tissues were subfractionated into nuclear and cytoplasmic fractions as described in MATERIALS AND METHODS, and 20 μg of total protein/lane were analyzed by Western immunoblot. Data are representative of  $n = 3$  rats.

(reviewed in Ref. 3). This view has been recently brought into question by *in vitro* studies showing significant non-nuclear PARP-1 activity (34), as well as activation by DNA structures lacking DNA breaks but associated with development (35). Consistent with this emerging concept of increased complexity, our results show that PARP-1 exhibits marked ontogenic changes in abundance, cellular distribution, and subcellular localization,

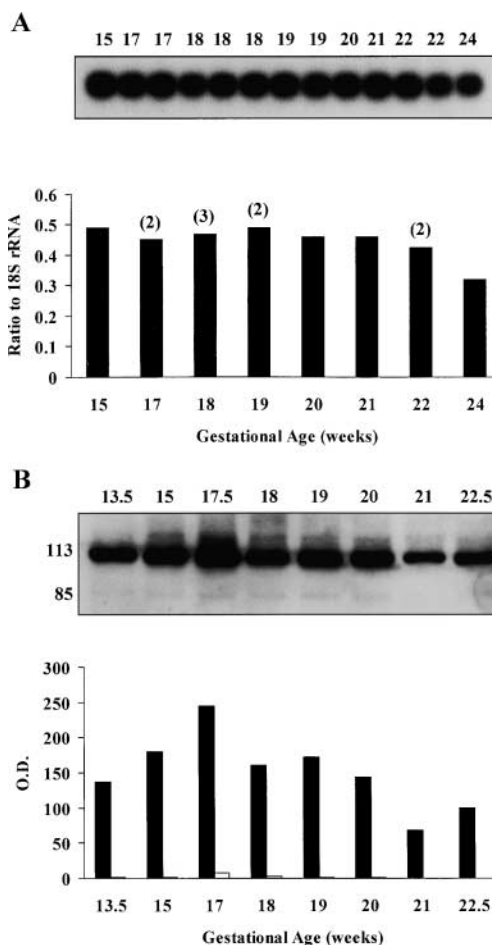
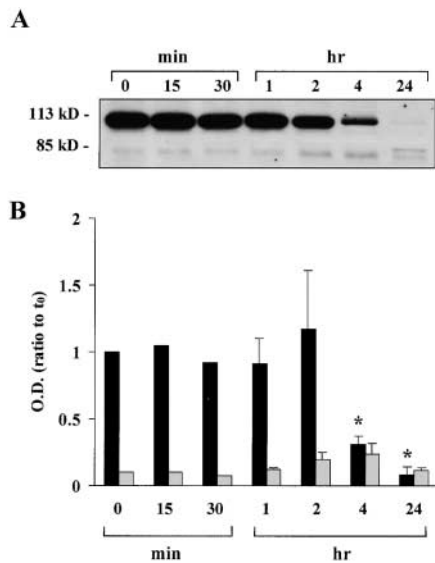


Figure 7. PARP-1 expression in human fetal lung from 15–24 wk gestation. (A) mRNA detected by RT-PCR and analyzed by optical densitometry. A quantity of 0.250 μg of total RNA was subjected to Multiplex RT-PCR for PARP-1 and 18S with primer and Competimer ratios as described in MATERIALS AND METHODS. Values are normalized to 18S rRNA. Data are representative of three different autoradiographs. Numbers in parentheses indicate  $n$  values as shown in blot. (B) Protein detected by Western immunoblot and analyzed by optical densitometry. Thirty micrograms of total protein/lane were subjected to electrophoresis on SDS-10% PAGE, transferred, and immunoblotted. Values are relative densitometric units. Filled bars, 113 kD; shaded bars, 85 kD.



**Figure 8.** PARP-1 protein content in human fetal lung explant culture detected by Western immunoblot. (A) Time course of PARP-1 content from a 17-wk HFL in explant culture. Forty micrograms of total protein/lane were subjected to electrophoresis on SDS-10% PAGE, transferred, and immunoblotted. Data are representative of three experiments. (B) Optical densitometry analysis of Western blots. Values are expressed as ratio of time in culture to 0 h control and are means  $\pm$  SE;  $n = 3$  HFLs, except for 15 and 30 min where  $n = 1$ . Filled bars, 113 kD; shaded bars, 85 kD. \* $P < 0.05$  compared with time zero.

in differential regulation as p113 and p85, and in expression of cytoplasmic p85, previously associated with apoptosis (2). In addition, the maximal expression of PARP-1 in late fetal life, and the effect of the modulation of its activity on SP expression, suggest an involvement for PARP-1 in lung differentiation.

PARP-1 protein showed marked developmental changes both by Western blot and by immunohistochemistry. In RFL at Embryonic Day 16, PARP-1 was expressed mainly in peripheral lung parenchyma and in epithelial tubules, regions associated with cell proliferation in pseudoglandular lung (36), as well as dividing cells (Figure 4A), findings consistent with previous observations *in vitro* of upregulation of PARP-1 in dividing cells (9). In proliferating acute promyelocytic leukemia cells PARP-1 regulates cell cycle progression (6). By Western immunoblot, p113 content was high at Embryonic Days 16 and 18, decreased sharply at Embryonic Day 20, and then progressively decreased through adulthood; p85 content was constant during fetal development and showed a decrease postnatally (Figures 1A and 1B). By immunohistochemistry, PARP-1 staining was most intense at Embryonic Day 18 with almost all cells showing intense nuclear staining and moderate cytoplasmic staining (Figure 1B). By Embryonic Day 20, there was still intense nuclear staining of epithelial cells but interstitial cells showed reduced staining (Figure 2C). On initial examination of Figure 2, there appears to be more intense staining at Embryonic Day 20 (Figure 2C) than at Embryonic Day 16 (Figure 1B). This apparent conflict with the data in Figure 1 is due to two factors. (i) In the Western immunoblot, PARP-1 is normalized to total protein, and the lung protein concentration at Embryonic Day 16 is much lower than at Embryonic Day 20. Therefore, the immunohistochemical signal is less intense at Embryonic Day 16. (ii) Careful inspection of Figure 2C reveals that many of the nuclei (especially interstitial cells) do not express PARP-1.

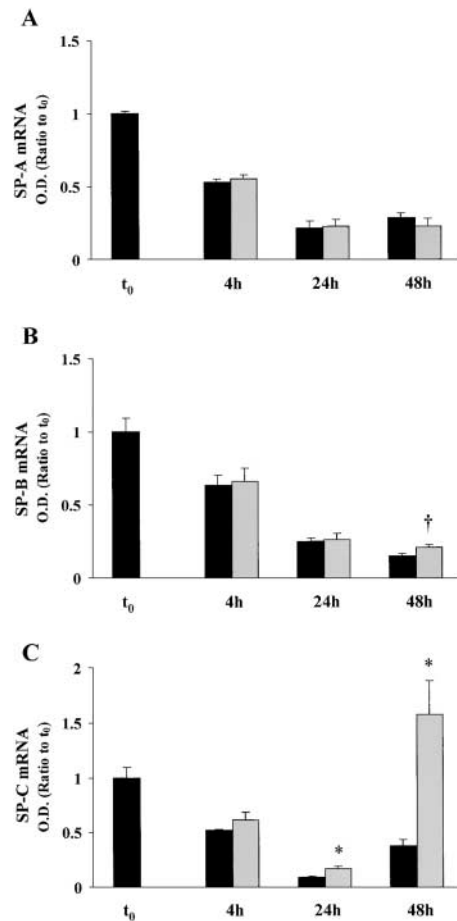


**Figure 9.** Effects of the PARP-1 inhibitor, INH<sub>2</sub>BP (200  $\mu$ M), on SP-A, -B, and -C mRNA expression in explant culture of Embryonic Day 21 fetal rat lung. Total lung RNA (0.25  $\mu$ g) was subjected to Multiplex RT-PCR for target gene and 18S with primer and Competimer ratios as described in MATERIALS AND METHODS. Values are normalized to 18S rRNA. Optical densitometry analysis is shown for (A) SP-A, (B) SP-B, and (C) SP-C. Values are normalized to the respective 0 h and are means  $\pm$  SD;  $n = 3$ . \* $P < 0.02$  and † $P = 0.05$  compared with control. Filled bars, control; shaded bars, INH<sub>2</sub>BP.

Immunolocalization showed that PARP-1 expression became progressively more restricted with maturation, so that fewer cells expressed PARP-1, whereas those that continued to express it did so at relatively high levels. The high PARP-1 expression at ed18 corresponds with the onset of terminal differentiation of the gas exchange epithelium (36, 37). This finding is consistent with results from the adipocyte (12) and chick limb differentiation models (11), in which predifferentiation peaks in PARP-1 expression and activity were demonstrated. Several proteins involved during differentiation in remodeling chromatin, and in transcriptional and post-transcriptional events, have been shown to be poly(ADP-ribosyl)ated (3, 38). Recently, Butler and Ordahl demonstrated that PARP-1 binds to specific muscle gene elements and activates the transcription factor that binds the same site and activates transcription (10). They hypothesized that PARP-1 integrates the two levels of control of gene expression, remodeling of chromatin and activation of gene transcription, to produce cell-specific gene expression in striated muscle (10).

We observed a marked developmental subcellular shift in

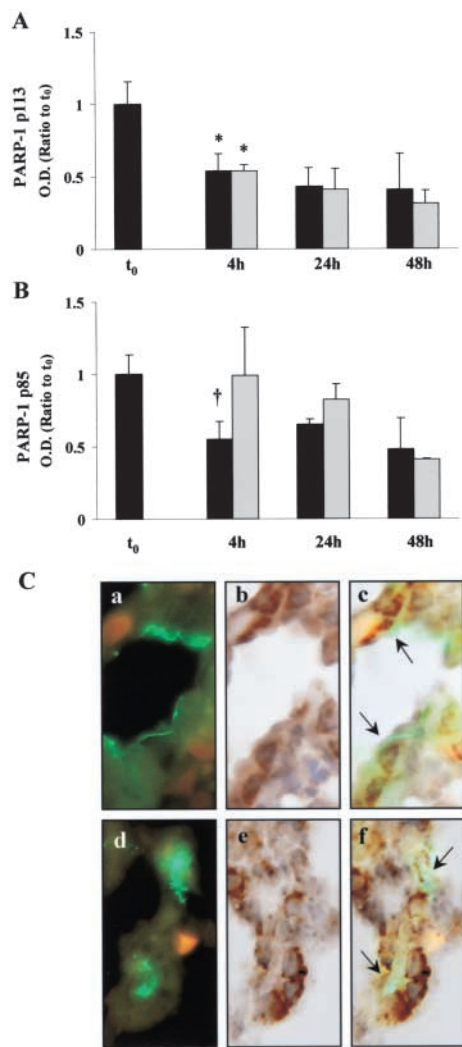


**Figure 10.** The effect of the specific PARP-1 inhibitor INH<sub>2</sub>BP (200  $\mu$ M) on PARP-1 protein content and localization in explant culture of Embryonic Day 21 fetal rat lungs. Optical density of Western blots are shown for p113 (A) and for p85 (B) at 0, 4, 24, and 48 h in culture. Data are shown as a ratio to time 0 and are expressed as mean  $\pm$  SE;  $n = 3$ , except for INH<sub>2</sub>BP at 4 h, where  $n = 2$ . \* $P < 0.05$  compared with time 0; † $P < 0.02$  compared with time 0. None of the differences between Control and INH<sub>2</sub>BP explants is significant. (C) Immunofluorescent (green) localization of RTII<sub>70</sub>, a protein specific in lung to the apical membrane of alveolar type II cells (a, d), immunohistochemical staining (brown) of PARP-1 (b, e), and composite photomicrograph of serial sections (c, f) of fetal rat lung explants cultured for 48 h. Control, a, b, c; cultures with INH<sub>2</sub>BP, d, e, f. Note that both RTII<sub>70</sub> and PARP-1 co-localize to the same cells. Filled bars, control; shaded bars, INH<sub>2</sub>BP.

PARP-1 localization from nucleus at Embryonic Day 18 to cytoplasmic granules at Postnatal Day 1 and in adult rats in airway epithelial cells (Figure 3). Although the cytoplasmic staining was more prominent, PARP-1 was also detectable in nuclei in postnatal lung. Cytoplasmic localization for PARP-1 has been previously reported in a subset of CNS motor neurons (39). A recent report described PARP-1 activity that was more abundant in mitochondria than nuclei of primary cortical neuron cultures in response to oxidative stress (34). In addition, cytoplasmic distribution has been observed for other ADP-ribosylating family members, including tankyrase and vPARP (2, 40). The role of PARP-1 in cytoplasmic perinuclear granules remains to be

defined. Experiments are underway to test the hypothesis that cytoplasmic PARP-1 provides a readily available reserve in cells that are likely to be exposed to environmental factors that could cause cellular damage (17, 18, 41).

Although PARP-1 in RFL began to progressively decrease at Embryonic Day 20, there was increased expression of PARP-1 in smooth muscle cells, primarily in cytoplasm, starting in late gestation and continuing postnatally (Figures 3 and 4). In contrast to the granular and perinuclear appearance in airway epithelial cells, PARP-1 in smooth muscle cells was distributed in regular, linear patterns throughout the cytoplasm. Althaus and associates showed that poly(ADP-ribose) inhibits the formation of actin filaments and suggested that this happens through binding to MARCKS proteins, which regulate the organization of the actin cytoskeleton (42). In *Drosophila*, overexpression of PARP-1 disrupted organization of cytoskeletal F-actin and tissue polarity (43). Thus, it is possible that cytoplasmic PARP-1 may play a role in cytoskeletal organization in the lung.

The relative abundance of PARP-1 as p113 and p85 in RFL changed with development. In mid-gestation, p85 was present at lower levels than p113, whereas in late gestation and postnatally, p85 was comparable in abundance to p113. In a previous study, Stiles and associates described the content of PARP-1, both p113 and p85, in fetal rats from Embryonic Day 15 to Embryonic Day 21. They reported that p113 content was more abundant than p85, except at Embryonic Day 18 and Embryonic Day 21 when there were marked increases in p85 and a marked decrease in p113 at Embryonic Day 21 (44). We did not detect the changes that they described (*see* Figure 1). Stiles and associates suggested that these changes at Embryonic Days 18 and 21 were secondary to apoptosis (44). In that report, the methods used for sample selection, protein solubilization, and the antibodies used for PARP-1 detection were different from those used in the present experiments. Therefore, technical reasons may explain the differences between the two studies. In prototypical models of apoptotic cell death, as p113 decreases due to cleavage by caspase-3, p85 increases proportionately (2). Therefore, some of the p85 content we observed is consistent with previous observations that apoptosis is part of normal development in both fetal (20) and neonatal lung (31–33). We observed that in RFL p113 content decreased significantly in late gestation, but without a proportional increase in p85 (Figures 1A and 1B). A possible explanation for these findings is that the dynamics of cleavage of p113 and of the clearance of p85 *in vivo* are different, and simple measurement of tissue levels of the two forms of PARP-1 is not indicative of these dynamics. However, other results in our study suggest that p85 may have a functional role. Subcellular fractionation showed that the cytoplasmic signal was due to p85 (Figure 6). In addition, immunohistochemical studies showed that there was abundant cytoplasmic PARP-1 localization in cells not known to undergo apoptosis in developing lung (*i.e.*, smooth muscle cells, Figures 3B and 4B) (9, 24, 30, 32). As noted above, the cytoplasmic appearance of PARP-1 differs in different cell types, granular in epithelial cells and diffusely throughout the cytoplasm in smooth muscle cells. These findings indicate the need for further studies (*i*) to identify and characterize possible nonapoptotic mechanism(s) that produce p85, and (*ii*) to define its possible cytoplasmic function(s). In support of these possibilities are the facts that p85 retains basal poly(ADP-ribosyl)ating function in the absence of the DNA binding domain (4, 45), and that inhibiting caspase-mediated cleavage of PARP-1 into p85 in *Drosophila* results in disrupted tissue polarity during development but has no effect on apoptosis (43).

HFL showed relatively constant expression of PARP-1 both at the level of mRNA and protein during the period examined (13.5–24 wk), with a modest decreasing trend in mRNA and

protein levels in the second half (Figure 7). In HFL explant culture, PARP-1 content decreased rapidly after 1 h and was minimally detectable at 24 h (Figure 8). PARP-1 content decreased in fetal rat lung in explant culture (Figures 10A and 10B), although the decrease was not as marked as in HFL. In explant cultures of human and rat fetal lung as well as in developing rat lung *in vivo* (Figures 1A and 1B), the marked reduction in p113 content was not accompanied by a corresponding increase in the p85 product, as would be expected if apoptosis were the sole mechanism by which p113 were degraded.

Previous results from *in vitro* models have shown that blocking poly (ADP-ribosyl)ation after the onset of differentiation can accelerate the rate of subsequent differentiation (reviewed in Ref. 3). This effect is believed to derive from the elimination of a repressive effect of PARP-1 activity that becomes evident once the differentiated state has been established (3). In Embryonic Day 21 lung, PARP-1 was localized to alveolar type II cells (Figure 10), and blocking PARP-1 activity with INH<sub>2</sub>BP affected expression of SP mRNAs (Figure 9). These effects ranged from no change in SP-A, to a modest increase in SP-B and a marked upregulation of SP-C. These different effects, with the addition of a specific PARP-1 inhibitor on the expression of SP-A, SP-B, and SP-C mRNA, imply differential regulation of the SP genes. During development, the three SPs undergo differential expression, with SP-C mRNA upregulation first, followed by SP-B and then SP-A (46). In addition, exogenous agents that accelerate SP expression, such as glucocorticoid and retinoic acid, also produce differential expression of SPs (46, 47). Further studies will be necessary to clarify the mechanisms involved in the differential regulation of SPs by PARP-1.

In summary, we have observed marked changes during development in lung expression of PARP-1 and in the cellular and subcellular distribution of this protein. Furthermore, the addition of the PARP-1 specific inhibitor, INH<sub>2</sub>BP, to explant cultures of fetal rat lung differentially affects expression of SP mRNAs. These findings indicate the possibility of important physiologic roles for PARP-1 in lung development. Further studies will be required to define these possible roles and their mechanisms of action.

**Acknowledgments:** The authors thank Drs. C. Ordahl and E. Kun for helpful suggestions. These studies were supported by National Heart, Lung and Blood Institute Grant HL-24075 and Child Health Research Center Grant P30-HD-28825.

## References

- Whitacre, C. M., H. Hashimoto, M. L. Tsai, S. Chatterjee, S. J. Berger, and N. A. Berger. 1995. Involvement of NAD-poly(ADP-ribose) metabolism in p53 regulation and its consequences. *Cancer Res.* 55:3697-3701.
- Kickhoefer, V. A., A. C. Siva, N. L. Kedersha, E. M. Inman, C. Ruland, M. Streuli, and L. H. Rome. 1999. The 193-kD vault protein, VPARP, is a novel poly(ADP-ribose) polymerase. *J. Cell Biol.* 146:917-928.
- Althaus, F. R., and C. Richter. 1987. ADP-ribosylation of proteins. Enzymology and biological significance. *Mol. Biol. Biochem. Biophys.* 37:1-237.
- Uchida, K., and M. Miwa. 1994. Poly(ADP-ribose) polymerase: structural conservation among different classes of animals and its implications. *Mol. Cell Biochem.* 138:25-32.
- Shall, S. 1984. Inhibition of DNA repair by inhibitors of nuclear ADP-ribosyl transferase. *Nucleic Acids Symp. Ser.* 13:143-191.
- Dantzer, F., H. P. Nasheuer, J. L. Vonesch, G. de Murcia, and J. Menissier-de Murcia. 1998. Functional association of poly(ADP-ribose) polymerase with DNA polymerase alpha-primase complex: a link between DNA strand break detection and DNA replication. *Nucleic Acids Res.* 26:1891-1898.
- Simbulan-Rosenthal, C. M., D. S. Rosenthal, A. H. Boulares, R. J. Hickey, L. H. Malkas, J. M. Coll, and M. E. Smulson. 1998. Regulation of the expression or recruitment of components of the DNA synthesome by poly(ADP-ribose) polymerase. *Biochemistry* 37:9363-9370.
- Bhatia, M., J. B. Kirkland, and K. A. Meckling-Gill. 1996. Overexpression of poly(ADP-ribose) polymerase promotes cell cycle arrest and inhibits neutrophilic differentiation of NB4 acute promyelocytic leukemia cells. *Cell Growth Differ.* 7:91-100.
- McNerney, R., M. Tavasoli, S. Shall, A. Brazinski, and A. Johnstone. 1989. Changes in mRNA levels of poly(ADP-ribose) polymerase during activation of human lymphocytes. *Biochim. Biophys. Acta* 1009:185-187.
- Butler, A. J., and C. P. Ordahl. 1999. Poly(ADP-ribose) polymerase binds with transcription enhancer factor 1 to MCAT1 elements to regulate muscle-specific transcription. *Mol. Cell. Biol.* 19:296-306.
- Cherney, B. W., R. J. Midura, and A. I. Caplan. 1985. Poly(ADP-ribose) synthetase and chick limb mesenchymal cell differentiation. *Dev. Biol.* 112:115-125.
- Smulson, M. E., V. H. Kang, J. M. Ntambi, D. S. Rosenthal, R. Ding, and C. M. Simbulan. 1995. Requirement for the expression of poly(ADP-ribose) polymerase during the early stages of differentiation of 3T3-L1 preadipocytes, as studied by antisense RNA induction. *J. Biol. Chem.* 270:119-127.
- Berger, N. A. 1985. Poly(ADP-ribose) in the cellular response to DNA damage. *Radiat. Res.* 101:4-15.
- Ha, H. C., and S. H. Snyder. 1999. Poly(ADP-ribose) polymerase is a mediator of necrotic cell death by ATP depletion. *Proc. Natl. Acad. Sci. USA* 96:13978-13982.
- Miwa, M., S. Hanai, P. Poltronieri, M. Uchida, and K. Uchida. 1999. Functional analysis of poly(ADP-ribose) polymerase in *Drosophila melanogaster*. *Mol. Cell Biochem.* 193:103-107.
- de Murcia, J. M., C. Niedergang, C. Trucco, M. Ricoul, B. Dutrillaux, M. Mark, F. J. Oliver, M. Masson, A. Dierich, M. LeMeur, C. Walztinger, P. Chambon, and G. de Murcia. 1997. Requirement of poly(ADP-ribose) polymerase in recovery from DNA damage in mice and in cells. *Proc. Natl. Acad. Sci. USA* 94:7303-7307.
- Wang, Z. Q., B. Auer, L. Stingl, H. Berghammer, D. Haidacher, M. Schweiger, and E. F. Wagner. 1995. Mice lacking ADPRT and poly(ADP-ribosyl)ation develop normally but are susceptible to skin disease. *Genes Dev.* 9:509-520.
- Wang, Z. Q., L. Stingl, C. Morrison, M. Jantsch, M. Los, K. Schulze-Osthoff, and E. F. Wagner. 1997. PARP is important for genomic stability but dispensable in apoptosis. *Genes Dev.* 11:2347-2358.
- Shieh, W. M., J. C. Ame, M. V. Wilson, Z. Q. Wang, D. W. Koh, M. K. Jacobson, and E. L. Jacobson. 1998. Poly(ADP-ribose) polymerase null mouse cells synthesize ADP-ribose polymers. *J. Biol. Chem.* 273:30069-30072.
- Scavo, L. M., R. Ertsey, C. J. Chapin, L. Allen, and J. A. Kitterman. 1998. Apoptosis in the development of rat and human fetal lungs. *Am. J. Respir. Cell Mol. Biol.* 18:21-31.
- Tewari, M., L. T. Quan, K. O'Rourke, S. Desnoyers, Z. Zeng, D. R. Beidler, G. G. Poirier, G. S. Salvesen, and V. M. Dixit. 1995. Yama/CPP32 beta, a mammalian homolog of CED-3, is a CrmA-inhibitable protease that cleaves the death substrate poly(ADP-ribose) polymerase. *Cell* 81:801-809.
- Gonzales, L. W., P. L. Ballard, R. Ertsey, and M. C. Williams. 1986. Glucocorticoids and thyroid hormones stimulate biochemical and morphological differentiation of human fetal lung in organ culture. *J. Clin. Endocrinol. Metab.* 62:678-691.
- Ertsey, R., C. J. Chapin, J. A. Kitterman, and L. M. Scavo. 2000. Poly(ADP-ribose) polymerase is expressed in fetal lung and is developmentally regulated. *Pediatr. Res.* 47:68A. (Abstr.)
- Bauer, P. I., E. Kirsten, G. Varadi, L. J. T. Young, A. Hakam, J. A. Comstock, and E. Kun. 1995. Reversion of malignant phenotype by 5-iodo-6-amino-1,2-benzopyrone a non-covalently binding ligand of poly(ADP-ribose) polymerase. *Biochimie* 77:374-377.
- Acarregui, M. J., J. M. Snyder, and C. R. Mendelson. 1993. Oxygen modulates the differentiation of human fetal lung in vitro and its responsiveness to cAMP. *Am. J. Physiol.* 264:L465-L474.
- Scavo, L. M., R. Ertsey, and B. Q. Gao. 1998. Human surfactant proteins A1 and A2 are differentially regulated during development and by soluble factors. *Am. J. Physiol.* 275:L653-L669.
- Duriez, P. J., S. Desnoyers, J. C. Hoflack, G. M. Shah, B. Morelle, S. Bourassa, G. G. Poirier, and B. Talbot. 1997. Characterization of anti-peptide antibodies directed towards the automodification domain and apoptotic fragment of poly (ADP-ribose) polymerase. *Biochim. Biophys. Acta* 1334:65-72.
- Yoshizawa, J., C. J. Chapin, L. Sbragia, R. Ertsey, J. A. Gutierrez, C. T. Albanese, and J. A. Kitterman. 2003. Tracheal occlusion stimulates cell cycle progression and type I cell differentiation in lungs of fetal rats. *Am. J. Physiol.* 285:L344-L353.
- Bohinski, R. J., R. Di Lauro, and J. A. Whitsett. 1994. The lung-specific surfactant protein B gene promoter is a target for thyroid transcription factor 1 and hepatocyte nuclear factor 3, indicating common factors for organ-specific gene expression along the foregut axis. *Mol. Cell. Biol.* 14:5671-5681.
- Gutierrez, J. A., R. Ertsey, L. M. Scavo, E. Collins, and L. G. Dobbs. 1999. Mechanical distention modulates alveolar epithelial cell phenotypic expression by transcriptional regulation. *Am. J. Respir. Cell Mol. Biol.* 21:223-229.
- Bruce, M. C., C. E. Honaker, and R. J. Cross. 1999. Lung fibroblasts undergo apoptosis following alveolarization. *Am. J. Respir. Cell Mol. Biol.* 20:228-236.
- Kresch, M. J., C. Christian, F. Wu, and N. Hussain. 1998. Ontogeny of apoptosis during lung development. *Pediatr. Res.* 43:426-431.
- Schittny, J. C., V. Djonov, A. Fine, and P. H. Burri. 1998. Programmed cell death contributes to postnatal lung development. *Am. J. Respir. Cell Mol. Biol.* 18:786-793.

34. Du, L., X. Zhang, Y. Y. Han, N. A. Burke, P. M. Kochanek, S. C. Watkins, S. H. Graham, J. A. Carcillo, C. Szabo, and R. S. Clark. 2003. Intra-mitochondrial poly-ADP-ribosylation contributes to NAD<sup>+</sup> depletion and cell death induced by oxidative stress. *J. Biol. Chem.* 278:18426–18433.
35. Kun, E., E. Kirsten, and C. P. Ordahl. 2002. Coenzymatic activity of randomly broken or intact double-stranded DNAs in auto and histone H1 trans-poly(ADP-ribosylation), catalyzed by poly(ADP-ribose) polymerase (PARP I). *J. Biol. Chem.* 277:39066–39069.
36. Burri, P. H., and M. Moschopoulos. 1992. Structural analysis of fetal rat lung development. *Anat. Rec.* 234:399–418.
37. Burri, P. H. 1984. Fetal and postnatal development of the lung. *Annu. Rev. Physiol.* 46:617–628.
38. Rawling, J. M., and R. Alvarez-Gonzalez. 1997. TFIIF, a basal eukaryotic transcription factor, is a substrate for poly(ADP-ribosyl)ation. *Biochem. J.* 324:249–253.
39. Cookson, M. R., P. G. Ince, P. A. Usher, and P. J. Shaw. 1999. Poly(ADP-ribose) polymerase is found in both the nucleus and cytoplasm of human CNS neurons. *Brain Res.* 834:182–185.
40. Smith, S., and T. de Lange. 1999. Cell cycle dependent localization of the telomeric PARP, tankyrase, to nuclear pore complexes and centrosomes. *J. Cell Sci.* 112:3649–3656.
41. Trucco, C., F. J. Oliver, G. de Murcia, and J. Menissier-de Murcia. 1998. DNA repair defect in poly(ADP-ribose) polymerase-deficient cell lines. *Nucleic Acids Res.* 26:2644–2649.
42. Althaus, F. R., H. E. Kleczkowska, M. Malanga, C. R. Muntener, J. M. Pleschke, M. Ebner, and B. Auer. 1999. Poly ADP-ribosylation: a DNA break signal mechanism. *Mol. Cell Biochem.* 193:5–11.
43. Uchida, M., S. Hanai, N. Uematsu, K. Sawamoto, H. Okano, M. Miwa, and K. Uchida. 2002. Overexpression of poly(ADP-ribose) polymerase disrupts organization of cytoskeletal F-actin and tissue polarity in *Drosophila*. *J. Biol. Chem.* 277:6696–6702.
44. Stiles, A. D., D. Chrysis, H. W. Jarvis, B. Brighton, and B. M. Moats-Staats. 2001. Programmed cell death in normal fetal rat lung development. *Exp. Lung Res.* 27:569–587.
45. Smith, S. 2001. The world according to PARP. *Trends Biochem. Sci.* 26:174–179.
46. Mendelson, C. R. 2000. Role of transcription factors in fetal lung development and surfactant protein gene expression. *Annu. Rev. Physiol.* 62:875–915.
47. Bogue, C. W., H. C. Jacobs, D. W. Dynia, C. M. Wilson, and I. Gross. 1996. Retinoic acid increases surfactant protein mRNA in fetal rat lung in culture. *Am. J. Physiol.* 271:L862–L868.